

Stellar mass loss and the Intra-Cluster Medium in Galactic globular clusters: a deep radio survey for HI and OH

Jacco Th. van Loon^{1*}, Snežana Stanimirović², A. Evans¹ and Erik Muller^{3,4}

¹*Astrophysics Group, School of Physical & Geographical Sciences, Keele University, Staffordshire ST5 5BG, United Kingdom*

²*Radio Astronomy Lab, University of California at Berkeley, 601 Campbell Hall, Berkeley CA 94720, USA*

³*Arecibo Observatory, National Astronomy and Ionosphere Center, HC3 Box 53995, Arecibo PR 00612, USA*

⁴*CSIRO Australia Telescope National Facility, PO Box 76, Epping NSW 1710, Australia*

Submitted 2005

ABSTRACT

We present the results of a survey, the deepest to date, for HI emission at 21 cm and OH emission at 18 cm (lines at 1612, 1665, 1667 and 1720 MHz) in the direction towards the Galactic globular clusters M 15, M 2, NGC 6934, NGC 7006 and Pal 13. The aim is to measure the amount of hydrogen in the intra-cluster medium (ICM), and to find OH masers in the circumstellar envelopes of globular cluster red giants. We present a tentative detection of 0.3 M_{\odot} of neutral hydrogen in M 15 and possible detections of neutral hydrogen in M 2 and Pal 13. We derive upper limits to the neutral hydrogen content of NGC 6934 and NGC 7006. No OH emission is detected. We also present deep HI data of the northern tip of the Magellanic Stream behind Pal 13.

Key words: circumstellar matter – ISM: atoms – ISM: molecules – globular clusters: general – radio lines: ISM – radio lines: stars

1 INTRODUCTION

Globular clusters (GCs) contain red giants, both first ascent Red Giant Branch (RGB) stars and Asymptotic Giant Branch (AGB) stars. These red giants have evolved from 0.8–1 M_{\odot} main-sequence stars, and are believed to lose 10–20 per cent of their mass on the RGB and a similar amount on the AGB before ending as low-mass white dwarfs. This mass loss is induced by radial stellar pulsation, and further driven by radiation pressure on dust grains that form in the cool, dense atmosphere. The GC’s Intra-Cluster Medium (ICM) is thus continuously replenished with neutral material. The wind outflow velocities are with $v_{\text{wind}} \sim 10 \text{ km s}^{-1}$ smaller than the escape velocity $v_{\text{esc}} \sim 20\text{--}50 \text{ km s}^{-1}$ of a typical GC. Hence of order 100 M_{\odot} of interstellar material must have accumulated within the GC (Tayler & Wood 1975) before it is removed by ram pressure upon crossing the Galactic plane, which typically happens once every $\sim 10^8 \text{ yr}$ (Odenkirchen et al. 1997).

Circumstellar dust has been found around red giants in the GCs M 15, M 54, NGC 362, NGC 6388, ω Cen and 47 Tuc (Ramdani & Jorissen 2001; Origlia et al. 2002). Origlia et al. (1997) possibly detected CO emission from Mira variables in ω Cen. Further evidence for stellar mass loss in GC red giants includes blue-asymmetric absorption line profiles in optical spectra (Bates, Kemp & Montgomery 1993), H α line

emission (Cohen 1976) which however is complicated by the presence of a chromosphere (Dupree, Hartmann & Smith 1990), and stellar pulsation and associated levitation of the stellar atmosphere (Frogel, Persson & Cohen 1981; Frogel & Elias 1988). In addition, 4 Planetary Nebulae (PNe) have been found in as many GCs (Jacoby et al. 1997).

However, the ICM has been more elusive.

Dust: Dust comprises at most one per cent of the mass, but it is easily detected. IR observations (IRAS, ISO) placed upper limits of $M_{\text{dust}} \sim 10^{-3} M_{\odot}$ (Lynch & Rossano 1990; Knapp, Gunn & Connolly 1995; Origlia, Ferraro & Fusi Pecci 1996; Hopwood et al. 1999). Observations at mm wavelengths yield similar limits (Penny, Evans & Odenkirchen 1997), with a possible detection of $M_{\text{dust}} \sim 10^{-2} M_{\odot}$ in the metal-rich GC NGC 6356 (Hopwood et al. 1998). The only secure detection, $M_{\text{dust}} \sim 5 \times 10^{-4} M_{\odot}$ of cold dust was found in the metal-poor GC M 15 (Evans et al. 2003).

Molecular gas: CO is a good tracer of molecular gas, which is mostly in the form of H₂, but attempts to detect CO yielded upper limits of $M_{\text{gas}} \sim 0.1 M_{\odot}$ (Smith, Woodsworth & Hesser 1995; Leon & Combes 1996; Hopwood 2001), with a possible detection at a similar level in 47 Tuc (Origlia et al. 1997). Searches for OH 1612 MHz maser emission (Knapp & Kerr 1973; Frail & Beasley 1994) only produced foreground sources, and no H₂O masers have been found (Cohen & Malkan 1979). The most sensitive OH search to date, in the 1665+7 MHz main lines at Arecibo by Dickey & Malkan (1980), resulted in no detection.

* E-mail: jacco@astro.keele.ac.uk

Atomic gas: Faulkner et al. (1991) detected neutral hydrogen (H I) at 21 cm in NGC 2808 and inferred the presence of $M_{\text{gas}} \sim 200 M_{\odot}$, but other attempts to detect H I have so far resulted in upper limits of only a few M_{\odot} (e.g., Knapp, Rose & Kerr 1973; Smith et al. 1990) — down to as little as $\sim 0.3 M_{\odot}$ in the most sensitive searches performed at Arecibo (Birkinshaw, Ho & Baud 1983; H I detected near M 56 is probably associated with intervening material).

Ionized gas: Hot stars such as blue horizontal branch stars or post-AGB stars produce a radiation field with $T_{\text{rad}} > 10,000$ K, which might ionize the ICM. Searches for free-free continuum or H α line emission have set limits of $M_{\text{gas}} \sim 1 M_{\odot}$ (Knapp et al. 1996: VLA, 8.4 GHz; Faulkner & Freeman 1977; Smith, Hesser & Shawl 1976; Hesser & Shawl 1977; Grindlay & Liller 1977). On the other hand, the presence of a population of free electrons in 47 Tuc is inferred from pulsar timing observations (Freire et al. 2001).

We have performed a new, sensitive search at Arecibo in the 21 cm H I transition and, in parallel, in all four 18 cm OH transitions, to investigate the atomic and molecular content of the ICM and to search for circumstellar OH masers within a small selection of Galactic GCs.

2 OBSERVATIONS

2.1 Radio L-band spectroscopy

The Arecibo radio telescope¹ was used between 17 and 23 September 2004 with the L-wide receiver to measure the H I line at 1420 MHz, the OH mainlines at 1665 and 1667 MHz and the OH satellite lines at 1612 and 1720 MHz in the direction of a selection of Galactic GCs (Table 1).

Each of the four boards of the correlator was centered on one of the lines’ laboratory frequency, with board 3 being centered on 1666.38 MHz in between the two OH main lines. The correlator was set for 9-level interleave sampling at two orthogonal polarizations, using a bandwidth of 6.25 MHz for the H I and 3.125 MHz for the OH lines. The four spectra, obtained with 1-sec integration dumps, were sampled with 1024 channels, resulting in a channel width of 1.29 and 0.57–0.53 km s⁻¹ for the H I and OH 1612–1720 MHz lines, respectively.

The system temperature was typically 26–28 K at 1420 MHz, at a gain of ~ 10 K Jy⁻¹. Calibration from correlator counts to the antenna temperature units was performed with respect to the noise diode (“hcal”) of known strength. The system was validated at the start of the first night through the observation of the bright circumstellar OH maser emission from the Galactic star RX Sge.

We followed a standard ON/OFF position switching strategy, pointing alternately at the centre of the target and at a “blank sky” position, while tracking exactly the same azimuth and zenith angle range for both ON and OFF scans. Typical integration time per scan was 5 min, followed by an ON/OFF observation of the noise diode for 10 sec. The total accumulated on-target integration times are listed in Table 2. As an additional experiment, to better sample the

emission from intervening matter, we also performed sparse mapping of M 15, M 2 and Pal 13 by obtaining ON spectra at 6–8 positions around the target’s centre separated by 3.5 arcmin. Note that the FWHM for the L-wide receiver is 3.4 arcmin at a frequency of 1420 MHz, and 2.9 arcmin at a frequency of 1666 MHz (Heiles et al. 2001, with updates on <http://www.naic.edu/~phil/sysperf/sysperf.html>).

The spectra were processed in IDL, using standard Arecibo routines to calibrate the individual ON and OFF spectra (<http://www.naic.edu/~phil/>). The combined OFF spectrum was smoothed by 7 channels (H I) or 15 channels (OH), respectively, to provide a reference which is practically noise free but which still contains all of the slow baseline structure. The baseline-corrected spectra were then derived by taking the difference between the combined ON spectrum and this reference.

2.2 Target selection

The targets were selected from the Harris (1996: revision 22 June 1999) catalogue of 147 Galactic GCs, with $-1 < \text{Declination} < +36$ deg and Galactic latitude $|b_{\text{II}}| > 18$ deg. Some of their properties are summarised in Table 1. Both M 15 and M 2 are massive GCs with large tidal radii, and any ICM may therefore be distributed over many arcminutes. However, most of the stellar mass is well confined within the Arecibo beam of $\sim 3'$, with M 15 having experienced core collapse, and any ICM must also be centrally concentrated to some degree. The GCs NGC 6934 and NGC 7006 have large velocities with respect to the Galactic disk, minimising the risk of contamination with foreground emission.

M 15 is given the highest priority since circumstellar dust (Origlia et al. 2002) and intra-cluster dust (Evans et al. 2003) have been detected in it, as well as the PN Ps 1 (Alves, Bond & Livio 2000 and references therein). The high central velocity dispersion of ~ 10 to 15 km s⁻¹ is interpreted by some as evidence for the presence of an intermediate-mass black hole (Gerssen et al. 2002), although recent N-body models do not require such a black hole (McNamara, Harrison & Anderson 2003).

It has been argued that the small GC Pal 13 is in the process of being tidally disrupted unless it is dark-matter dominated (Siegel et al. 2001; Côté et al. 2002). Blecha et al. (2004) measure a systemic velocity of $v_{\text{LSR}} = 32.2 \pm 0.4$ km s⁻¹ and a radial velocity dispersion of $\sigma_v = 0.9 \pm 0.3$ km s⁻¹. Côté et al. show evidence for the velocity dispersion to rise from < 1 km s⁻¹ in the cluster core to ~ 3 km s⁻¹ (i.e. comparable to the escape velocity) at a projected distance of 1.4' from the core.

3 RESULTS

We analysed the “total” ON–OFF spectrum and, where applicable, the difference between the total ON spectrum and (only) the combined spectra taken at the offset pointings in the sparse map. We shall refer to the latter as the “mapping” spectrum, whilst the “pointing” spectrum refers to the standard ON/OFF position switching mode excluding the sparse map offset pointings.

¹ The Arecibo Observatory is part of the National Astronomy and Ionosphere Center, operated by Cornell University under a cooperative agreement with the National Science Foundation.

Table 1. The observed GCs, with parameters from Harris (1996: revision 22 June 1999) unless otherwise indicated. Listed are: name, equatorial (J2000) and Galactic coordinates, distance d_{\odot} to the Sun, reddening E_{B-V} , systemic velocity v_{LSR} with respect to the Local Standard of Rest, central radial velocity dispersion σ_{rad} , central escape velocity v_{esc} (from Webbink 1985), metallicity $[\text{Fe}/\text{H}]$ with respect to solar, and the core radius r_{core} , half-mass radius $r_{M/2}$ and tidal radius r_{tidal} . References are as follows: a=Blecha et al. (2004); b=Côté et al. (2002); c=Gerssen et al. (2002); d=McNamara et al. (2003); e=Pryor et al. (1986); f=Siegel et al. (2001); g=Webbink (1985).

Object	RA 2000 (h m s)	Dec 2000 ($^{\circ}$ $'$ $''$)	l_{II} ($^{\circ}$)	b_{II} ($^{\circ}$)	d_{\odot} (kpc)	E_{B-V} (mag)	v_{LSR} (km s $^{-1}$)	σ_{rad}	v_{esc}	$[\text{Fe}/\text{H}]$	r_{core}	$r_{M/2}$	r_{tidal}
												(arcmin)	
NGC 6934	20 34 11.6	7 24 15	52.10	-18.89	17.4	0.09	-396.7 \pm 1.6	5 ^g	22	-1.54	0.25	0.60	8.4
NGC 7006	21 01 29.5	16 11 15	63.77	-19.41	41.5	0.05	-369.7 \pm 0.4	4 ^g	17	-1.63	0.24	0.38	6.3
M 15	21 29 58.3	12 10 01	65.01	-27.31	10.3	0.10	-94.8 \pm 0.2	13 ^{c,d}	41	-2.25	0.07	1.06	21.5
M 2	21 33 29.3	-0 49 23	53.38	-35.78	11.5	0.06	5.1 \pm 2.0	8 ^e	37	-1.62	0.34	0.93	21.5
Pal 13	23 06 44.4	12 46 19	87.10	-42.70	24.8 ^f	0.05	30.4 \pm 0.5 ^b	2 ^{a,b}	3	-1.65	0.48	0.46	2.2

3.1 Measuring the ICM mass

To convert measured brightness temperature into gas mass, one has to first consider whether the emission is spatially resolved. To estimate the expected radial extent of a cool ICM, we assume hydrostatic equilibrium:

$$\frac{dp}{dr} = -\rho_{\text{gas}} \frac{GM}{r^2}, \quad (1)$$

where the gas has a pressure p and density ρ_{gas} , and the gravitational potential is due to stellar mass M enclosed by radius r . Assuming an ideal, isothermal gas of temperature T , and using the Poisson equation for the stars, we obtain:

$$\rho_{\star} = -\frac{kT}{4\pi Gm} \nabla^2 \ln \rho_{\text{gas}}, \quad (2)$$

where the gas molecules have a mass m . We approximate the stellar mass density, ρ_{\star} , by a singular isothermal sphere:

$$\rho_{\star}(r) = \rho_{\star}(r_0) (r_0/r)^2. \quad (3)$$

Here r_0 is an arbitrary reference point for which we take the half-mass radius, $r_{M/2}$. By simple integration we obtain the density at that point, $\rho_{\star}(r_{M/2})$, as a function of half-mass radius and total stellar mass, M_{\star} . Solving Eq. (2) for the gas density we obtain:

$$\rho_{\text{gas}} \propto r^{-\alpha}, \quad (4)$$

where the exponent is given by:

$$\alpha = \frac{GmM_{\star}}{2kTr_{M/2}}. \quad (5)$$

For typical values of $M_{\star} = 10^5 M_{\odot}$, $r_{M/2} = 10^{17}$ m and $m \sim 2 \times 10^{-27}$ kg, the gas density profile follows exactly that of the stars if $T \sim 5,000$ K. Cooler gas will sink deeper into the core. We thus conclude that the atomic or molecular ICM is not expected to be resolved as the Arecibo beam is a few times larger than the half-mass radii of our target clusters.

We thus employ the usual formula (e.g., Braun & Burton 2000) to find the neutral hydrogen mass per beam:

$$M_{\text{H}}[M_{\odot}] = 0.024 d_{\odot}^2 \int T_{\text{B}}(v) dv, \quad (6)$$

where the cluster distance, d_{\odot} , is in kpc, the brightness temperature, T_{B} , is in K and the velocities, v , are in km s $^{-1}$. We adopt a main beam efficiency of 0.7 to convert antenna temperature units into a brightness

Table 2. On-target integration times (pointing plus mapping) and rms noise levels per beam. H I rms values for M 2 and Pal 13 refer to the difference spectrum with respect to the sparse mapping offset pointings (Figs. 2 & 3).

Object	t_{int} (min)	H I		OH	
		σ_{T} (mK)	σ_{M} (M_{\odot})	σ_{T} (mK)	σ_{F} (mJy)
NGC 6934	58	5.5	0.15	6.8	0.7
NGC 7006	48	6.6	0.9	7.5	0.8
M 15	100+30	3.3 [†]	0.05	4.9	0.5
M 2	10+25	29.8	0.43	9.7	1.0
Pal 13	25+20	10.1	0.34	8.7	0.9

[†] rms = 1.4 mK in the smoothed $\times 6$ spectrum of Fig. 1.

temperature scale (Heiles et al. 2001, with updates on <http://www.naic.edu/~phil/sysperf/sysperf.html>).

The rms noise, σ_{T} (in antenna temperature), was computed in 50–100 km s $^{-1}$ spectral intervals at one or either side of the GC velocity, excluding 20 km s $^{-1}$ centred at the GC velocity and avoiding obvious signal. The noise can then be converted into the equivalent mass per beam:

$$\sigma_{\text{M}}[M_{\odot}] = 0.034 d_{\odot}^2 \sigma_{\text{T}} (\Delta v \sigma_{\text{rad}})^{\frac{1}{2}}, \quad (7)$$

where the channel width, Δv , and radial velocity dispersion, σ_{rad} , are in km s $^{-1}$. Noise levels are listed in Table 2.

3.2 Neutral hydrogen

In Fig. 1 the H I spectrum in the direction of the core of M 15 is displayed, together with a smoothed version obtained with a 6-channel running boxcar. H I emission is detected at precisely the velocity of M 15. The emission is resolved from the Galactic foreground emission, which only interferes at $v_{\text{LSR}} > -80$ km s $^{-1}$. The width of the emission is similar to the radial velocity dispersion of M 15, lending further support to the reality of the detection. The integrated emission corresponds to a neutral hydrogen mass of $M_{\text{H}} \simeq 0.3 M_{\odot}$, which is significant at a level of more than 5σ . Much less integration time was spent in mapping mode than in pointing mode and the sparse map of M 15 cannot therefore reveal a similarly weak signal as that shown in Fig. 1.

In Figs. 2 & 3 are displayed the H I spectra of M 2 and Pal 13, together with the “pointing” OFF spectrum and the individual offset pointings in the sparse map. If the same

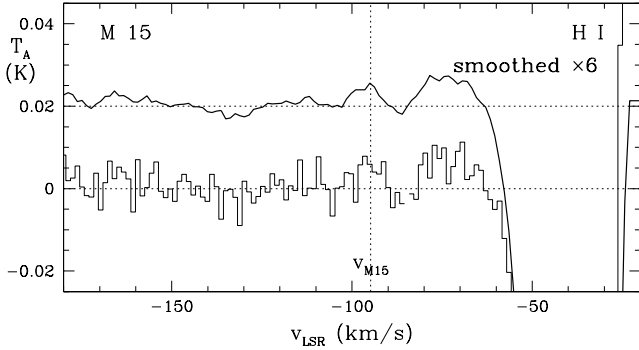


Figure 1. H I 21 cm spectrum towards M15 (histogram). A smoothed version of the spectrum is created by using a running boxcar of 6 channels, and displayed with a vertical offset for clarity. With an original channel width of 1.29 km s^{-1} the smoothed spectrum has a velocity resolution of 8 km s^{-1} . A vertical line indicates the systemic velocity of M15, $v_{\text{LSR}} = -94.8 \text{ km s}^{-1}$. Located outside of the Galactic foreground emission (which is here negative after subtraction of brighter emission in the OFF beam) is a faint peak of emission centred at the velocity of M15.

offset pointing was revisited then the individual spectra were averaged. The middle panel shows the difference between the ON spectrum and the combined OFF pointings from the sparse map, along with the standard deviation (σ) amongst these OFF pointings. In the bottom panel this ON–OFF spectrum is expressed in terms of σ to show the significance of excess emission in the core of the GC as compared to the fluctuations in the surrounding emission.

For M2 the sparse mapping may have allowed us to detect H I in its core despite the strong Galactic foreground emission: the core has excess emission over surrounding pointings at a velocity of $v_{\text{LSR}} = +3 \text{ km s}^{-1}$ (Fig. 2), which is within the 2 km s^{-1} uncertainty of the velocity of M2. The emission reaches a nearly 4σ significance over fluctuation in the surrounding emission. Another peak of excess emission at $v_{\text{LSR}} = +10 \text{ km s}^{-1}$ does not appear to be significant as the same emission component is seen in the S and NW offset pointings. Given the large tidal radius of M2 it is still possible that this emission is extended and physically associated with the cluster. The $+3 \text{ km s}^{-1}$ component seems to reside in the core of M2, and would correspond to a neutral hydrogen mass of $M_{\text{H}} \approx 3 M_{\odot}$.

The radial velocity of Pal13 places it on the wing of strong Galactic foreground emission. However, that emission varies very little across the sparse map, and as a result there is a hint of extremely faint emission at $v_{\text{LSR}} = +33 \text{ km s}^{-1}$ at a 2σ level and much stronger excess emission at $v_{\text{LSR}} \approx +5 \text{ km s}^{-1}$ (Fig. 3). Although the latter reaches a significance of over 3σ with respect to the surrounding emission fluctuations, this component suffers from much greater Galactic contamination. Its large velocity difference of $\Delta v \approx -25 \text{ km s}^{-1}$ casts doubt on a physical association with Pal13 as it exceeds the escape velocity by almost an order of magnitude. Excess emission is, however, seen at all velocities from ~ 0 up to $\sim 40 \text{ km s}^{-1}$, and the two “components” only become separate when expressing their strengths in σ .

Emission from the Magellanic Stream behind Pal13 was detected at $v_{\text{LSR}} \approx -382 \text{ km s}^{-1}$ (see Appendix A), and an

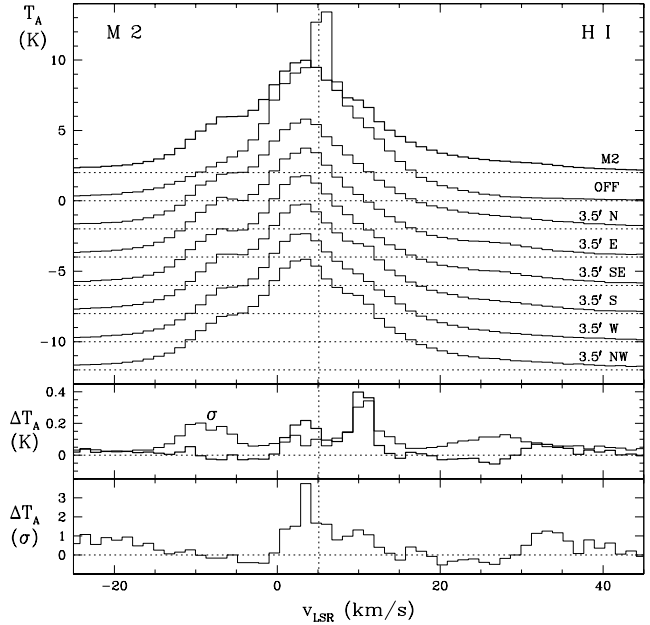


Figure 2. H I 21 cm spectrum towards M2 (top panel, boldface). Below that are displayed the position switching OFF spectrum and the six spectra obtained at the individual OFF pointings in the sparse map. The spectra are offset with respect to each other for clarity. In the middle panel are displayed the M2 spectrum after subtracting the combined spectrum of the OFF pointings in the sparse map (boldface) and the rms amongst the sparse mapping OFF pointings (σ , thin line). Their ratio is displayed in the bottom panel. A vertical line indicates the systemic velocity of M2, $v_{\text{LSR}} = 5.1 \text{ km s}^{-1}$. The channel width is 1.29 km s^{-1} . There is a hint of emission at 3 km s^{-1} centred at M2, and at 10 km s^{-1} but without showing a central concentration.

intermediate-velocity cloud can be seen in the OFF beam at $v_{\text{LSR}} \approx -50 \text{ km s}^{-1}$ (Fig. 3).

No H I was detected in NGC 6934 or NGC 7006, despite the very low noise levels and large systemic velocities. The $5\text{-}\sigma$ upper limit to the neutral hydrogen mass in the Arecibo beam is $M_{\text{H}} < 0.8 M_{\odot}$ for NGC 6934, somewhat smaller than the upper limit obtained by Birkinshaw et al. (1983). For NGC 7006 the $5\text{-}\sigma$ upper limit is $M_{\text{H}} < 5 M_{\odot}$. Given their small projected sizes it is unlikely that a significant amount of neutral hydrogen mass was missed.

3.3 Hydroxyl

No OH emission was detected from any of the GCs in our sample, neither in the main lines nor in the satellite lines. Dickey & Malkan (1980) observed NGC 7006, M15 and Pal13 at 1665 and 1667 MHz at rms levels that correspond to 6.6, 3.9 and 4.4 mJy for our velocity channel width: our search is 5–8 times more sensitive (Table 2). Frail & Beasley (1994) obtained upper limits to the 1612 MHz emission at an equivalent rms level of $\sim 60 \text{ mJy}$. Our search was more sensitive than this by two orders of magnitude.

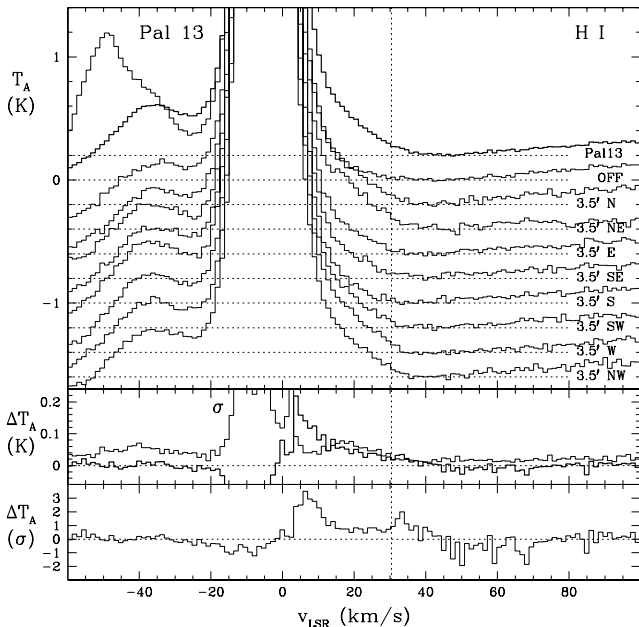


Figure 3. H I 21 cm spectrum towards Pal 13, displayed in a similar way as Fig. 2, but now there are eight OFF pointings in the sparse map and the systemic velocity of Pal 13 is $v_{\text{LSR}} = 30.4 \text{ km s}^{-1}$. There is a hint of centrally concentrated emission at 5 and 33 km s^{-1} and possibly in between, but the Galactic foreground emission interferes strongly.

4 DISCUSSION

4.1 The globular cluster ICM

The deepest H I survey to date was performed at Arecibo by Birkinshaw et al. (1983). Not only is the new L-wide receiver more sensitive, but also Birkinshaw et al. observed known radio sources at generally more than a beam-width *away from the GC centre*. They will thus have missed gas residing within the GC core. Pointing directly at the GC centres and performing sparse mapping observations to remove Galactic foreground emission greatly improved our chances of detecting the ICM.

We detect H I emission in the core of M 15. The excellent agreement between the peak velocity and velocity dispersion of the H I emission and those of M 15 strongly suggest that the neutral hydrogen in M 15 is associated with the ICM. It is unlikely to be associated with the PN Ps 1 in M 15, as the velocity of Ps 1 differs from that of M 15 by $> 20 \text{ km s}^{-1}$ (Rauch, Heber & Werner 2002). The cold dust detected in M 15 by Evans et al. (2003) is almost certainly associated with the ICM (rather than being of circumstellar nature) and the neutral hydrogen may be directly associated with this dust component.

The H I emission detected in at least one (M 15) and possibly up to three (M 2 and Pal 13) out of five GCs indicates that the ICM typically contains $M_{\text{H}} \lesssim 1 M_{\odot}$ of neutral hydrogen (of course, besides any hydrogen there must be at least another 25 per cent in the form of helium). This is roughly equivalent to the total amount of mass lost by a few low-mass AGB stars, which happens on a timescale of 10^6 yr . Stripping of the ICM during Galactic plane crossing occurs on timescales that are two orders of magnitude longer, and massive GCs such as M 2 and M 15 each contain

dozens of AGB stars. One would thus have expected to find more than two orders of magnitude more ICM than what we detect here in neutral hydrogen. This problem becomes even worse if we consider only 5- σ upper limits to our data, which correspond to $\sim 1 M_{\odot}$.

Freire et al. (2001) argue that the stellar radiation field in a GC is sufficient to ionize all hydrogen. They provide evidence for the presence of $M_{\text{H}} \simeq 0.1 M_{\odot}$ in the form of plasma, in 47 Tuc as well as in M 15. This is less than the mass of neutral hydrogen that we detect, and therefore insufficient to solve the missing ICM mystery.

More hydrogen may be hidden in molecular form. The gas-to-dust mass ratio in the circumstellar envelope of an AGB star is ~ 200 at solar metallicity, and scales approximately linearly with metallicity (van Loon et al. 2005). The detection of $5 \times 10^{-4} M_{\odot}$ of dust in M 15 (Evans et al. 2003), in combination with a gas-to-dust mass ratio of $\psi \sim 20,000$ for this metal-poor GC, would lead to a predicted $M_{\text{H}} \simeq 10 M_{\odot}$ of gas, the majority of which must therefore be in molecular form. Such large reservoirs of molecular gas are not supported by observations of CO, which yield upper limits on the total gas mass of $M_{\text{gas}} \sim 0.1 M_{\odot}$. The real gas-to-dust ratio is extremely uncertain, though. On the basis of the detected amount of neutral hydrogen alone, one would estimate $\psi \sim 600$ for the ICM of M 15.

There are indications for Pal 13 to be tidally disrupted (Siegel et al. 2001), a process which may already have removed gas from its ICM. If the H I emission in our spectrum of Pal 13 is real then its large velocity spread of $\Delta v \sim 30 \text{ km s}^{-1}$ compared to its stellar velocity dispersion and escape velocity of only 2–3 km s^{-1} might imply that we are witnessing the stripping of the gas from the GC. NGC 6934 and NGC 7006 are considerably more massive and tidal stripping at their current locations in the Galactic halo is expected to be much weaker than for the low-mass GC Pal 13. Still, our upper limits to the neutral hydrogen content of these two GCs are with a few M_{\odot} tight enough to require some stripping mechanism in addition to the passage through the Galactic plane. Especially NGC 7006 is quite distant from the galaxy and is therefore certain to have lived in relative isolation for the past 10^8 years.

Could a wind drive mass loss from the GC at a rate of $\dot{M}_{\text{GC}} \sim 10^{-6} M_{\odot} \text{ yr}^{-1}$? The wind speed in low-mass AGB stars is too low to overcome the gravitational pull of a typical GC. However, the combined stellar radiation field of the GC might be able to drive a wind for much longer, pushing the gas out to a distance at which the local gravitational acceleration has dropped sufficiently for the gas to become gravitationally unbound. At an outflow velocity of 10 km s^{-1} the gas would have been dispersed over more than the Arecibo beamsize within a few 10^5 yr for a GC at a distance of 10 kpc. For this to work, the gas must have sufficient opacity to be driven by radiation pressure. Although atomic and molecular hydrogen are extremely inefficient for this, they may be collisionally coupled with other sources of opacity such as dust grains or ions. It would have been easier to explain an absence of dust and an abundance of interstellar gas in this way as at low density the dust will be unable to drag the gas with it, but at least in the case of M 15 we do find ourselves in that situation.

Isolated dwarf irregular (dIrr) galaxies are more gas-rich than dIrrs within 250 kpc of the Milky Way or M 31, and

the gas-less dwarf spheroidal galaxies are almost exclusively found in the vicinity of either the Milky Way or M 31. This may be understood if ram pressure in a hot halo is effective in stripping the dIrrs of their gas (Blitz & Robishaw 2000). If true, then this could also be a viable mechanism for stripping GCs of their gas as their orbits never take them completely out of the galactic halo (Frank & Gisler 1976; Lea & De Young 1976).

4.2 Circumstellar masers in globular clusters

The envelopes of mass-losing AGB stars provide an ideal environment for OH masers to occur. The 18 cm transition can be pumped by the infrared radiation arising from the circumstellar dust, and the slow cool wind ensures a long velocity coherence path. The 1612 MHz line is normally the strongest maser in well-developed outflows, but the 1665 MHz line can dominate at low mass-loss rates when the OH is located closer to the warm stellar photosphere and the 1667 MHz line might be seen in circumstellar envelopes with short velocity coherence paths. Thermal emission is orders of magnitude weaker than the maser emission.

No maser emission was detected in any of the GCs that we looked at. Would we have expected to detect any circumstellar masers? Assuming the same scaling relation of the OH intensity with bolometric luminosity as found for the OH masers detected in the Galactic centre and Large Magellanic Cloud (Marshall et al. 2004), and assuming a bolometric magnitude of $-4 < M_{\text{bol}} < -3$ for a low-mass thermal-pulsing AGB star, then the expected intensity of the OH maser in a GC AGB star would be ~ 0.1 Jy at the distance of M 2 or M 15. That is more than an order of magnitude brighter than our $5\text{-}\sigma$ upper limits.

The OH maser mechanism in the metal-poor outflows of low-mass GC AGB stars may be less efficient due to the reduced infrared emission in a dust-poor wind. The OH masers may also be fainter due to a lower abundance of hydroxyl as a result of the lower abundance of oxygen and/or a higher photo-dissociation rate in the stronger and less attenuated stellar radiation field in a GC.

5 SUMMARY

We conducted the deepest survey to date, at H I 21 cm and OH 1612, 1665, 1667 and 1720 MHz with Arecibo, towards five Galactic globular clusters. We present a tentative detection of $0.3 M_{\odot}$ of neutral hydrogen in the core of M 15. This is a few orders of magnitude less than what is expected to accumulate via stellar mass loss, and a removal mechanism in addition to Galactic plane crossings is still required to explain the paucity of the intra-cluster medium.

No OH maser emission was detected in any of the clusters, at a level which is an order of magnitude below that expected from scaling known OH masers sources to the likely properties of mass-losing AGB stars in globular clusters. The faintness of globular cluster OH masers may be due to the low metallicity and strong interstellar radiation field.

ACKNOWLEDGMENTS

We would like to thank the telescope operators at Arecibo Observatory for their excellent support, Joana Oliveira for help with IDL and other matters, and Carl Heiles for reading the manuscript. We also thank the referee for her/his very helpful comments. Support by NSF grants AST-0097417 and AST-9981308 is gratefully acknowledged. SS appreciates the hospitality of the Keele Astrophysics Group during the observations.

REFERENCES

- Alves D.R., Bond H.E., Livio M. 2000, AJ 120, 2044
 Bates B., Kemp S.N., Montgomery A.S. 1993, A&AS 97, 937
 Birkinshaw M., Ho P.T.P., Baud B. 1983, A&A 125, 271
 Blecha A., Meylan G., North P., Royer F. 2004, A&A 419, 533
 Blitz L., Robishaw T. 2000, ApJ 541, 675
 Braun R., Burton W.B. 2000, A&A 354, 853
 Cohen J.G. 1976, ApJ 203, L127
 Cohen N.L., Malkan M.A. 1979, AJ 84, 74
 Côté P., Djorgovski S.G., Meylan G., Castro S., McCarthy J.K. 2002, ApJ 574, 783
 Dickey J.M., Malkan M.A. 1980, AJ 85, 145
 Dupree A.K., Hartmann L., Smith G.H. 1990, ApJ 353, 623
 Evans A., Stickel M., van Loon J.Th., Eyres S.P.S., Hopwood M.E.L., Penny A.J. 2003, A&A 408, L9
 Faulkner D.J., Freeman K.C. 1977, ApJ 211, 77
 Faulkner D.J., Scott T.R., Wood P.R., Wright A.E. 1991, ApJ 374, L45
 Frail D.A., Beasley A.J. 1994, A&A 290, 796
 Frank J., Gisler G. 1976, MNRAS 176, 633
 Freire P.C., Kramer M., Lyne A.G., Camilo F., Manchester R.N., D'Amico N. 2001, ApJ 557, L105
 Frogel J.A., Elias J.H. 1988, ApJ 324, 823
 Frogel J.A., Persson S.E., Cohen J.G. 1981, ApJ 246, 842
 Gerssen J., van der Marel R.P., Gebhardt K., Guhathakurta P., Peterson R.C., Pryor C. 2002, AJ 124, 3270
 Grindlay J.E., Liller W. 1977, ApJ 216, L105
 Harris W.E. 1996, AJ 112, 1487
 Heiles C., Perillat P., Nolan M., et al. 2001, PASP 113, 1247
 Hesser J.E., Shawl S.J. 1977, ApJ 217, L143
 Hopwood M.E.L. 2001, PhD thesis, Keele University
 Hopwood M.E.L., Evans A., Penny A., Eyres S.P.S. 1998, MNRAS 301, L30
 Hopwood M.E.L., Eyres S.P.S., Evans A., Penny A., Odenkirchen M. 1999, A&A 350, 49
 Jacoby G.H., Morse J.A., Fullton L.K., Kwitter K.B., Henry R.B.C. 1997, AJ 114, 2611
 Knapp G.R., Kerr F.J. 1973, AJ 78, 458
 Knapp G.R., Rose W.K., Kerr F.J. 1973, ApJ 186, 831
 Knapp G.R., Gunn J.E., Connolly A.J. 1995, ApJ 448, 195
 Knapp G.R., Gunn J.E., Bowers P.F., Vasquez Poritz J.F. 1996, ApJ 462, 231
 Lea S.M., De Young D.S. 1976, ApJ 210, 647
 Leon S., Combes F. 1996, A&A 309, 123
 Lynch D.K., Rossano G.S. 1990, AJ 100, 719
 Marshall J.R., van Loon J.Th., Matsuura M., Wood P.R., Zijlstra A.A., Whitelock P.A. 2004, MNRAS 355, 1348
 Mathewson D.S., Cleary J.D., Murray M.N. 1974, ApJ 190, 291
 McNamara B.J., Harrison T.E., Anderson J. 2003, ApJ 595, 187
 Odenkirchen M., Brosche P., Geffert M., Tucholke H.-J. 1997, New Astron. 2, 477
 Origlia L., Ferraro F.R., Fusi Pecci F. 1996, MNRAS 280, 572
 Origlia L., Gredel R., Ferraro F.R., Fusi Pecci F. 1997, MNRAS 289, 948

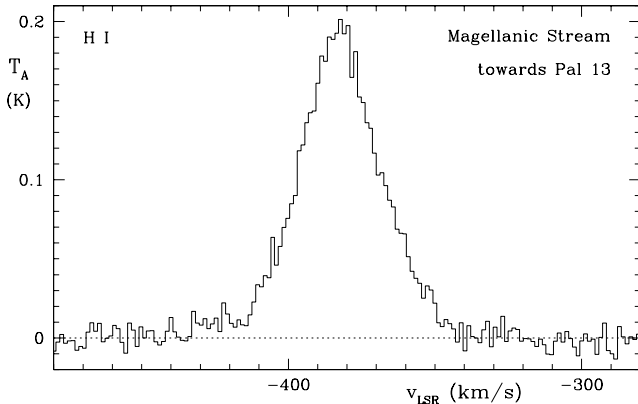


Figure A1. The Magellanic Stream detected in the H I 21 cm line in the direction of Pal 13. The spectrum is the result of 45 min on-source integration time, and a smoothed version of a featureless position-switching OFF spectrum has been subtracted to remove the baseline. The channel width is 1.29 km s^{-1} .

- Origlia L., Ferraro F.R., Fusi Pecci F., Rood R.T. 2002, ApJ 571, 458
- Penny A.J., Evans A., Odenkirchen M. 1997, A&A 317, 694
- Pryor C., McClure R.D., Fletcher J.M., Hartwick F.D.A., Kormendy J. 1986, AJ 91, 546
- Putman M.E., Staveley-Smith L., Freeman K.C., Gibson B.K., Barnes D.G. 2003, ApJ 586, 170
- Ramdani A., Jorissen A. 2001, A&A 372, 85
- Rauch T., Heber U., Werner K. 2002, A&A 381, 1007
- Siegel M.H., Majewski S.R., Cudworth K.M., Takamiya M. 2001, AJ 121, 935
- Smith M.G., Hesser J.E., Shawl S.J. 1976, ApJ 206, 66
- Smith G.H., Woodworth A.W., Hesser J.E. 1995, MNRAS 273, 632
- Smith G.H., Wood P.R., Faulkner D.J., Wright A.E. 1990, ApJ 353, 168
- Stanimirović S., Dickey J.M., Krčo M., Brooks A.M. 2002, ApJ 576, 773
- Tayler R.J., Wood P.R. 1975, MNRAS 171, 467
- van Loon J.Th., Cioni M.-R.L., Zijlstra A.A., Loup C. 2005, A&A in press
- Webbink R.F. 1985, in: Dynamics of star clusters, IAU Symposium 113. Reidel (Dordrecht), p541

APPENDIX A: THE NORTHERN TIP OF THE MAGELLANIC STREAM BEHIND PAL 13

H I emission from the Magellanic Stream (Mathewson, Cleary & Murray 1974) was detected behind Pal 13 (Fig. A1). This section corresponds to the northern tip of the stream, complex MS VI (Putman et al. 2003) and was studied in detail in Stanimirović et al. (2002). To our knowledge, our new observations represent the deepest H I data of the Magellanic Stream to date, comprising a total of 45 min on-source integration time and reaching an rms noise level well below 0.01 K. The baseline was removed by subtracting a smoothed version of the position-switching OFF spectrum, which itself was completely featureless apart from the slow baseline structure. The emission peaks at $v_{\text{LSR}} \simeq -382 \text{ km s}^{-1}$ and extends across $\sim 70 \text{ km s}^{-1}$.